Journal of Functional Materials and Applied Engineering

Research Paper

Optimization for Degradation of Antibiotics by Peroxyacetic Acid

Mittal Blouin[1,*], Fatih Farnood[1], Pooya Ozkan[1], Schott Leuschner[2], James Eduardo[2]

[1] Agroécologie, AgroSup Dijon, CNRS, INRA, University of Bourgogne Franche-Comté, F-21000, Dijon, France
[2] Nantes Université, Oniris, CNRS, GEPEA, UMR 6144, Saint-Nazaire F-44600, France
*Corresponding author: mittal.blouin@univ-nantes.fr

Abstract. Antibiotics are typical emerging micro-pollutants in the aquatic environment, characterized by persistence, high risk, potential unknown toxicity, and widespread residue. AOPs that exploit ·OH, $O_2^{\cdot-}$ and $SO_4^{\cdot-}$ have become a hot research topic for antibiotic wastewater because they are fast, versatile and highly efficient. Starting from the structural characteristics of antibiotics and combining density functional theory (DFT), this study systematically analyzes, for the first time, the attack sites and degradation mechanisms of different reactive species on five common categories of antibiotics. Zero-valent iron (Fe^0) was modified using the common aminopolycarboxylic acid (APCA) chelator EDTA via a liquid-phase impregnation method to construct an EDTA-Fe^0/Peroxyacetic Acid (PAA) catalytic system. Using the typical antibiotic sulfamethazine (SMT) as the target pollutant, this paper investigates the influence of modification parameters, system dosage, initial pH, and coexisting anions, aiming to reveal the enhanced activation mechanism of EDTA-Fe^0 within the system.

Keywords: *EDTA-modified zero-valent iron; Peroxyacetic acid; Antibiotic removal*

Received on 25 June 2024, Accepted on 28 August 2014, Published on 15 September 2014

1 Introduction

Widespread antibiotic consumption in livestock, farming, medicine and aquaculture has fueled the spread of antibiotic-resistance genes (ARGs) and resistant bacteria (ARB) in aquatic systems [1–2]. In contrast to conventional organics like dyes or pesticides, antibiotics—though present only in trace amounts—are acutely toxic and can trigger microbial resistance once released. Therefore, the effective removal of antibiotics from water bodies has become imperative.

Antibiotic-laden effluents can be tackled by physical adsorption, biological degradation or chemical oxidation [4–6]. Yet these traditional options are hampered by poor removal rates, high operating costs and secondary loads such as toxic by-products or heavy-metal residues, restricting their large-scale use [7]. Since Glaze et al. [8] proposed AOPs in 1987, which generate highly reactive species like ·OH and $SO_4^{\cdot-}$, they have played a crucial role in treating refractory wastewater [9-10]. Compared to traditional technologies, AOPs demonstrate significant advantages in antibiotic degradation, including strong oxidation capability, fewer secondary pollutants, and compact treatment footprint [11].

Modified Fe^0 technology is an efficient environmental remediation technique commonly used in wastewater treatment and soil/groundwater remediation. This approach relies on surface-functionalized Fe^0 particles that exhibit boosted adsorption and catalytic activity, accelerating redox steps for rapid organics destruction and heavy-metal conversion.In the field of environmental remediation, modified Fe^0 technology has been widely applied and shows great potential. The principle relies on Fe^0 particles acting as electron donors to participate in redox reactions with pollutants [12]. Additionally, modified Fe^0 exhibits higher reactivity and longer longevity, functioning effectively over a wider pH range, making it suitable for treating various types of wastewater [13]. Wastewater often contains diverse organic pollutants and heavy metal ions, posing serious threats to the environment and human health. Traditional water treatment methods are often inefficient and costly, whereas modified Fe^0 technology can efficiently degrade organic pollutants and transform heavy metal ions, elevating

wastewater treatment efficiency to a new level and providing an important guarantee for securing clean water resources [14].

Therefore, this study modifies Fe^0 using the liquid-phase impregnation method. Specifically, Fe^0 is modified with EDTA, a typical APCA containing four carboxyl groups and two amino groups, to construct two catalytic systems: EDTA-Fe^0/PAA and EDTA-Fe^0/H_2O_2. Using typical antibiotics SMT and tetracycline (TC) as target pollutants, the influence of modification parameters, system dosage, initial pH, and coexisting anions in both systems is investigated to reveal the enhanced activation mechanism of EDTA-Fe^0. Furthermore, Fe^0 modified with different APCA structures (EDTA, NTA, BCTA, etc.) is studied to elucidate the structure-activity relationship between APCA functional groups and the characterization properties of APCA-Fe^0.

2 Experimental Section

2.1 Reagents and Instruments

Zero-valent iron (Fe^0, ≥ 98 %), disodium EDTA (analytical grade), sulfamethazine (analytical grade), 30 % H_2O_2 (analytical grade), glacial acetic acid (HPLC grade), methanol (analytical grade) and tert-butanol (HPLC grade) were supplied by Shanghai Aladdin Biochemical Technology Co. Ltd. and Sigma-Aldrich LLC, respectively. Ultrapure water and deionized water obtained from a Biosafer-10R water purification system (Nanjing Saifei Biotechnology Co., Ltd.) were used throughout the experiments.

Additional reagents—HCl, NaOH, NaCl, $NaNO_3$, $NaHCO_3$, humic acid, 2,4-hexadiene, DMPO, 1,10-phenanthroline, H_3PO_4, MeOH (≥99.9 %), p-benzoquinone, benzoic acid, p-hydroxybenzoic acid, SMX, TC, BPA, SDZ, PMSO, $PMSO_2$ and PAA—were employed as received. SMT was obtained from Sinopharm Chemical Reagent Co., Ltd. (China).

PAA was prepared in-house by reacting HAc and H_2O_2 (volume ratio 3:2) with the addition of 3% H_2SO_4 as a catalyst. The suspension was magnetically stirred in the dark at ambient temperature for 24 h.

2.2 Experimental Procedures

For surface functionalization, 1 g of commercial Fe^0 powder was dispersed in 25 mL of 0.2 M EDTA solution. After 1 h of soaking, the powder was rinsed, filtered, and dried at 80 °C.

Degradation tests were carried out in 500 mL of reaction solution magnetically stirred at 350 rpm. SMT was spiked at 5 mg L^{-1}, and the pH was fine-tuned with 0.1 M HCl or NaOH. The reaction was started by introducing Fe^0 or EDTA-Fe^0 (0–0.3 g L^{-1}) together with PAA (0–1 mM). At preset intervals, 1 mL aliquots were withdrawn and instantly quenched with 0.5 mL MeOH. Each aliquot was then passed through a 0.22 μm syringe filter before instrumental analysis.

Systematic tests probed the effects of Fe^0/EDTA-Fe^0 load (0.05–0.3 g L^{-1}), pH (3–9.5), common anions (Cl^-, SO_4^{2-}, NO_3^-, HCO_3^-; 1–10 mM), humic acid (1–10 mM), and real water matrices. The contribution of radicals was assessed using radical scavenging experiments. This involved adding scavengers, including 1 M TBA, 1 M MeOH, and 5 mM 2,4-HD, to the solution before initiating the experiment.

2.3 Analytical Methods

Tafel curves were analyzed using an electrochemical workstation (CHI760E). A three-electrode cell was assembled with a glassy-carbon working electrode, Pt-wire counter, and saturated calomel reference (SCE) in 0.1 M Na_2SO_4. Polarization was recorded at 1 mV s^{-1}; TC concentration was monitored on a MAPADA P1 UV–vis spectrophotometer at 357 nm.

Dissolved Fe^{2+} and total iron were quantified colorimetrically with 1,10-phenanthroline, which forms an orange-red Fe(II)-tris-complex in acidic media. First, the sample solution was filtered to remove impurities. Then, an acetate-acetic acid buffer solution and 1,10-phenanthroline solution were added, mixed thoroughly, and

allowed to stand for 15 minutes for color development. Absorbance of the Fe(II)-phenanthroline complex was read at 510 nm on a UV–Vis spectrophotometer. To obtain total iron, hydroxylamine hydrochloride was first added to reduce any Fe^{3+} to Fe^{2+}, after which the identical colorimetric procedure was followed. The concentrations of Fe^{2+} or total iron were quantified by measuring the absorbance and using a standard curve or calculation formula. This method allows for accurate determination of dissolved Fe^{2+} and total iron concentrations, aiding in the analysis and control of iron content in samples.

Hydroxyl-radical levels were inferred from the BA → p-HBA conversion, since ·OH hydroxylates benzoic acid to p-hydroxybenzoic acid. The concentration of p-HBA can be accurately measured by HPLC. The concentration of ·OH was then calculated based on the quantitative relationship [15].

Fe(IV) was selectively tracked with methyl phenyl sulfoxide (PMSO), which is rapidly oxidized to methyl phenyl sulfone ($PMSO_2$) by Fe(IV). The amount of $PMSO_2$ generated was accurately measured by HPLC, and the Fe(IV) concentration was calculated based on the corresponding quantitative relationship. To measure Fe(IV), 0.5 mL of the sample was first quenched with dimethyl sulfoxide (DMSO) at designated time intervals. Exactly 1 mL of reaction liquor was pipetted into a centrifuge tube and clarified through a 0.22 μm organic-phase syringe filter. Finally, the filtered sample was analyzed under appropriate HPLC conditions to determine the Fe(IV) content accurately [16].

Structural models of Fe^0 and EDTA-Fe^0 were constructed. Reaction pathways and Gibbs-energy profiles for H_2O_2 (and by analogy PAA) activation over Fe^0 and EDTA-Fe^0 were computed with the Vienna Ab initio Simulation Package (VASP). Adsorption energies for H_2O_2 and *OOH on Fe^0 and EDTA-Fe^0, together with the corresponding values for PAA adsorption and its subsequent free-energy profile, were evaluated [17].

Following QSAR principles, the toxicities of TC, SMT and their transformation products were predicted with the Toxicity Estimation Software Tool (T.E.S.T.). Endpoints comprised developmental toxicity, mutagenicity, 48-h IGC_{50} against Tetrahymena pyriformis, and 96-h LC_{50} for fathead minnow.

3. Results and Discussion

3.1 Influence of Operational Conditions on SMT Degradation by the EDTA-Fe^0/PAA System

3.1.1 Effect of EDTA Concentration on EDTA-Fe^0 Performance

Figure 1 displays how varying EDTA loadings modulate the reactivity of the as-synthesized EDTA-Fe^0. Fe^0 was modified with 0, 0.05, 0.1, 0.2 and 0.4 M EDTA solutions, and the resulting materials were screened for SMT removal performance.The results indicate that SMT removal efficiency initially increased and then decreased with increasing EDTA concentration [18].

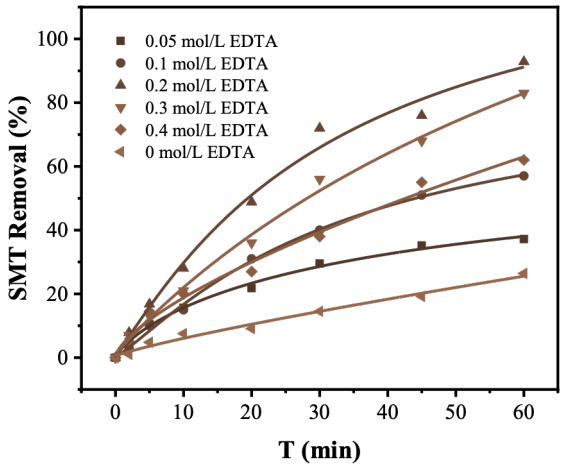

Figure 1 The effect of 3-4 different EDTA dosages on the removal of SMT by modified EDTA-Fe^0

Specifically, as the EDTA concentration increased from 0 M to 0.2 M, the SMT removal efficiency gradually improved. This suggests that an appropriate concentration of EDTA effectively promotes coordination on the Fe^0 surface, thereby enhancing reactivity [19]. However, when the EDTA concentration was further increased to 0.4 M, the SMT removal efficiency began to decline. This is likely because an excessively high EDTA concentration leads to the formation of abundant complexes, which may occupy the active sites on the Fe^0 surface, resulting in reduced reactivity. Consequently, 0.2 M was selected as the optimal EDTA concentration for preparing EDTA-Fe^0 [20]. This concentration sufficiently utilizes the coordination between EDTA and Fe^0 to improve reactivity while avoiding the adverse effects associated with high EDTA concentrations.

3.1.2 Effect of PAA Dosage

Close inspection of Figure 2a reveals that PAA dosage exerts a decisive influence on SMT abatement within the EDTA-Fe^0/PAA process. Raising PAA from 0.05 to 0.5 mM boosted SMT removal from 44.3 % to 97.0 % and the apparent rate constant from 0.021 to 0.121 min^{-1}. This upward trend reflects a higher steady-state concentration of oxidants at 0.5 mM PAA [21]; yet, pushing the dose to 1 mM marginally depressed both removal (96.3 %) and k (0.114 min^{-1}), signifying scavenging or self-quenching. This phenomenon may be attributed to an inhibitory effect caused by excess PAA, where some reactive species are consumed by PAA or adsorbed onto the EDTA-Fe^0 surface, hindering the dissolution of EDTA-Fe^0 and reducing the overall SMT removal efficiency.

Cross-comparing Figs. 2b–c confirms the EDTA-Fe^0/PAA couple markedly outperforms bare Fe^0/PAA in SMT degradation kinetics. At every identical PAA level, EDTA-Fe^0/PAA delivered both faster removal and higher pseudo-first-order rate constants than Fe^0/PAA [22]. At merely 0.05 mM PAA, EDTA-Fe^0/PAA attained 44.3 % SMT removal—surpassing the 28.2 % achieved by Fe^0/PAA even when the latter was supplied with ten-fold more oxidant (0.5 mM). This head-to-head comparison underscores the dominance of EDTA-Fe^0/PAA in SMT degradation [23] and demonstrates its capacity to match or exceed Fe^0/PAA performance while consuming far less oxidant. Specifically, the EDTA-Fe^0/PAA system enabled a reduction of over 90% in PAA usage, which is beneficial for lowering treatment costs and minimizing potential environmental impacts [24].

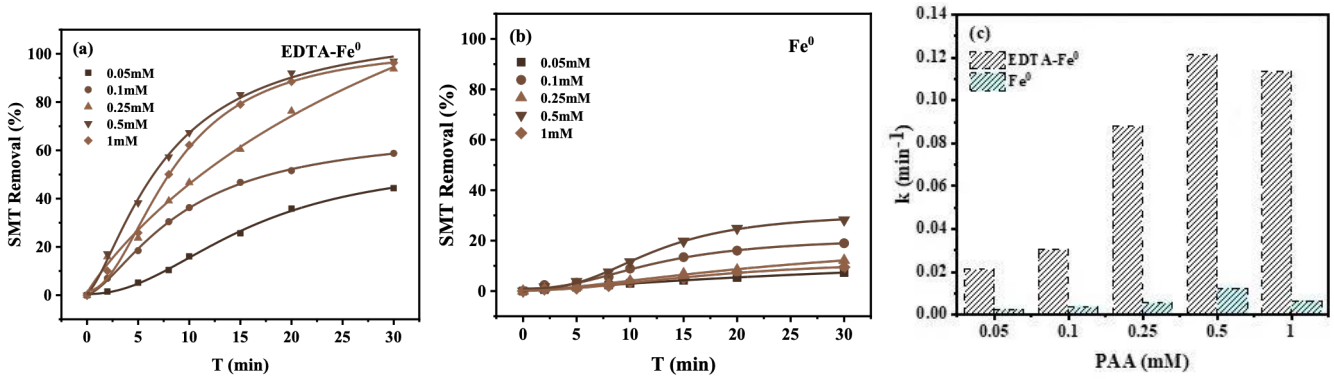

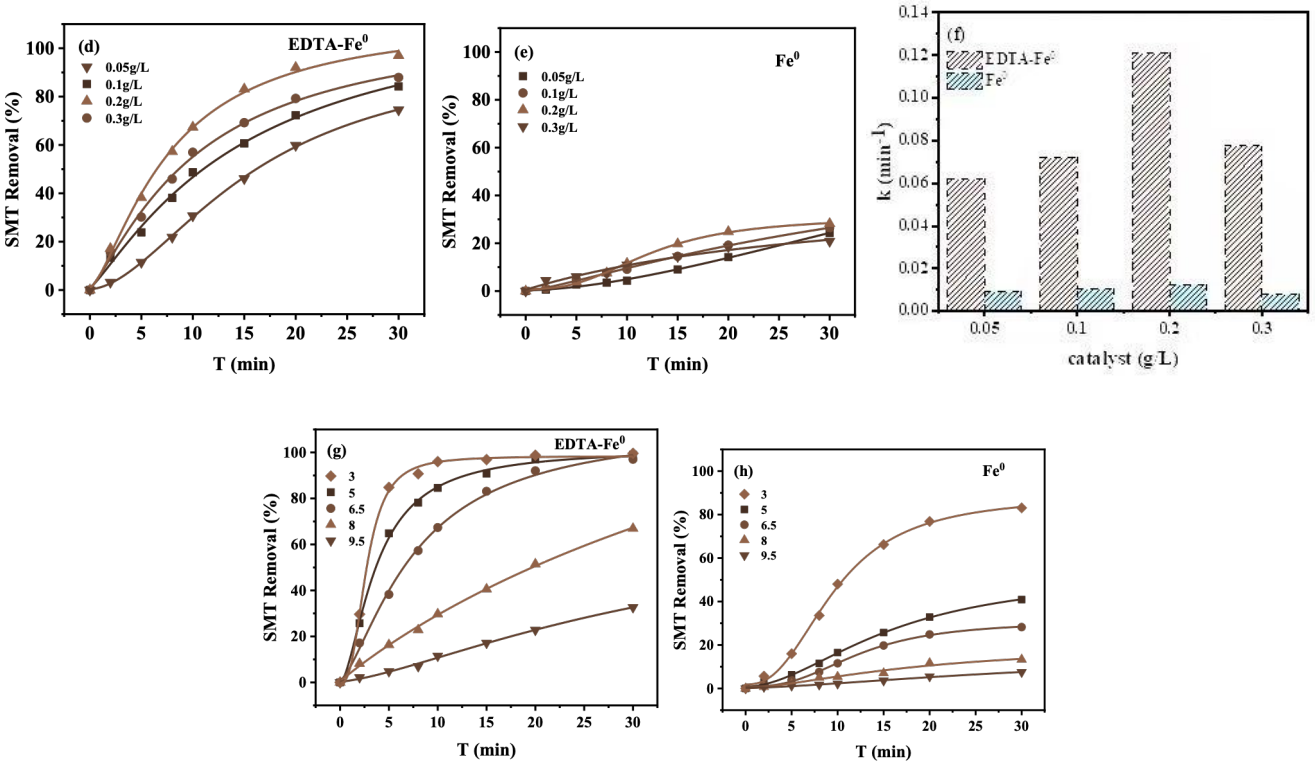

Figure 2 The removal efficiency and rate of SMT at different dosage of PAA in different systems (a-c); The removal efficiency and rate of SMT at different dosage of catalyst in different systems (d-f); The removal efficiency and rate of SMT at different pH in different systems (g-i). Reaction condition: SMT=5 mg/L, PAA=0.5 mM (except a-c), catalyst=0.2 g/L (except d-f), pH=6.5(except g-i) Reaction condition: SMT = 5 mg/L, catalyst = 0.2 g/L, PAA = 0.5 mM, pH = 6.5

3.1.3 Effect of Fe^o Dosage

Data analysis from Figure 2d reveals a significant influence of EDTA-Fe^o concentration on SMT removal efficiency. Boosting EDTA-Fe^o from 0.05 to 0.2 g L^{-1} lifted SMT removal from 74.5 % to 97.0 % and doubled the rate constant to 0.121 min^{-1}. This indicates that within this concentration range, increasing the EDTA-Fe^o dosage enhances the generation of reactive species in the system, thereby improving SMT removal. However, when the EDTA-Fe^o concentration was further increased to 0.3 g/L, the SMT removal efficiency decreased to 87.9%, and the k value dropped to 0.078 min^{-1}. This trend suggests that an excessive amount of EDTA-Fe^o may be detrimental to SMT removal. This could be due to the increased amount of dissolved iron from excess EDTA-Fe^o, which might excessively react with and consume the active radicals, reducing the degradation efficiency for SMT [25].

Across every Fe dose examined, Figures 2e–f reveal that EDTA-Fe^o/PAA consistently outperformed Fe^o/PAA in both SMT removal efficiency and reaction rate constants. EDTA markedly amplified the Fe^o–PAA synergy, enabling identical iron loadings to deliver superior SMT abatement. Relative to Fe^o/PAA, the EDTA-Fe^o/PAA process cuts iron usage by more than 70 % while maintaining equal or better SMT removal. This result underscores not only the economic benefit of the EDTA-Fe^o/PAA system but also its potential advantages in reducing environmental pressure and resource consumption [26].

3.1.4 Effect of Initial pH

Systematic pH scans were conducted to fully gauge how solution acidity affects EDTA-Fe^o/PAA performance in SMT elimination. Figure 2g shows that EDTA-Fe^o/PAA operates best under acidic pH: SMT removal declines steadily as the initial pH rises, reflecting the acid-promoted formation of reactive oxidants [27]. Even at neutral

pH (6.5), however, the system retained outstanding activity, erasing 97.0 % of SMT within 30 min. This robust neutral-pH performance evidences the broad applicability of EDTA-Fe^0/PAA, eliminating the need for costly acidification.

Across the entire pH window, the EDTA-Fe^0/PAA rate constant surpassed that of Fe^0/PAA by factors of 1.5–9.2 (Figs. 2h–i). This wide margin underscores the competitive edge of EDTA-Fe^0/PAA in SMT abatement, maintaining superiority regardless of pH drift.

In short, EDTA-Fe^0/PAA delivers peak performance in acid media yet retains high SMT-removal activity at neutral pH. This broad pH applicability endows the EDTA-Fe^0/PAA system with greater flexibility and potential for practical applications.

3.2 Toxicity Assessment of SMT Degradation Products

During EDTA-Fe^0/PAA treatment, SMT is successively transformed into a series of identifiable intermediates. Three plausible routes are postulated from the detected intermediates, illustrating a sequential SMT dismantling. Initial attack by ·OH/R-O· oxidants yields SMT1, SMT2 and SMT8. SMT2 arises from deeper oxidation of SMT1, and subsequent oxidation of SMT2 gives SMT3. In a parallel route, SMT8 rearranges to SMT9, whereas SMT6 emerges from an analogous rearrangement of the parent SMT, evidencing skeletal rearrangements throughout the degradation cascade. SMT7 is then generated by further oxidation of SMT6. Fission of the sulfonamide S–N linkage produces SMT4 and SMT5, a key step that breaks the antibiotic core. Importantly, SMT7 can additionally originate from SMT5 oxidation, revealing cross-talk among the three proposed pathways. Ultimately, all intermediates are attacked by the same oxidant pool and mineralized to harmless CO_2 and H_2O, accomplishing complete SMT degradation within the EDTA-Fe^0/PAA system. Mapping these pathways deepens mechanistic insight and furnishes a theoretical framework for tuning reaction conditions to boost degradation efficiency [27].

A full toxicity audit of SMT and its transformation products was therefore undertaken to gauge the environmental footprint of the EDTA-Fe^0/PAA process. Developmental and acute toxicities were quantified via the 48-h IGC_{50} against Tetrahymena pyriformis and the 96-h LC_{50} for fathead minnow, respectively. The evaluation results showed that the developmental toxicity values of SMT3, SMT4, SMT5, SMT6, and SMT7 were significantly lower than that of SMT itself. This finding indicates that these intermediates have a lesser toxic effect on organisms during the developmental stage, suggesting a lower environmental risk compared to SMT. Yet SMT1, SMT2, SMT8 and SMT9 showed marginally higher developmental toxicity, whereas their acute-toxicity endpoints (T. pyriformis 48-h IGC_{50} and fathead minnow 96-h LC_{50}) were all below the parent SMT values. Consequently, acute assays indicate these intermediates pose a diminished hazard to both T. pyriformis and fathead minnow relative to the parent antibiotic. Although a few transient products retain moderate activity, the overall EDTA-Fe^0/PAA treatment yields a less-toxic mixture, qualifying it as an environmentally sound option for SMT abatement. The process achieves efficient SMT mineralization without markedly increasing ecotoxicity.

3.3 Applicability of the EDTA-Fe^0/PAA System

Inorganic anions and humic acids—ubiquitous in real wastewater—often dictate the performance of Fe^0-driven AOPs. Their impact on EDTA-Fe^0/PAA was dissected in Figure 3a: Cl^-, SO_4^{2-} and NO_3^- left SMT removal virtually unchanged. These anions appear to interfere minimally with ·OH, R–O· and Fe(IV) formation, so the oxidant flux—and hence SMT removal—remains intact. In contrast, HCO_3^- noticeably slowed SMT elimination. This deceleration stems from ·OH scavenging by HCO_3^- to yield weaker HCO_3·/CO_3·$^-$ radicals; nevertheless, 79 % SMT was still removed, evidencing a compensating contribution from R–O· and Fe(IV). Although humic acid can compete for oxidants, EDTA-Fe^0/PAA showed robust tolerance, retaining high SMT removal even in HA-rich matrices. The high steady-state concentration of ·OH, R–O·, and Fe(IV) outcompetes HA scavenging, preserving rapid SMT degradation.

To probe versatility, the EDTA-Fe^0/PAA process was challenged with additional antibiotics (SDZ, TC, SMX) and the plasticizer BPA, each possessing distinct molecular architectures. Figure 3b shows EDTA-Fe^0/PAA greatly outperformed Fe^0/PAA in both removal extents and k values for every antibiotic, underscoring that EDTA-functionalization broadly amplifies degradability across diverse pharmaceutical structures. EDTA-Fe^0 therefore acts as a high-performance, broad-spectrum catalyst: paired with PAA it rapidly eliminates SDZ, TC, SMX and

BPA alike. These results offer clear guidance for scaling-up the EDTA-Fe^0/PAA technology to tackle mixed antibiotic residues in real wastewater matrices.

Cycling tests confirmed that EDTA-Fe^0 retains its activity over successive runs, evidencing robust recyclability. Across five reuse cycles (Fig. 3c), SMT removal stayed at 97.0 %, 97.0 %, 97.4 %, 92.9 % and 87.7 %, demonstrating sustained catalytic power and underscoring its practical merit. This durable, high-level performance guarantees operational reliability over prolonged use, lending strong techno-economic support for full-scale deployment.

Additionally, the influence of real water matrices on SMT degradation by EDTA-Fe^0/PAA was evaluated. As shown in Figure 3d, SMT removal in natural freshwater matched that in deionized water, evidencing broad matrix tolerance. In 30 min, EDTA-Fe^0/PAA eliminated 83.4 % of SMT from natural freshwater—four-fold higher than Fe^0/PAA (20.2 %)—confirming robust performance across diverse aqueous matrices. This matrix-independent activity highlights the system's stability and versatility, a critical asset for real-world treatment scenarios where feed-water composition varies.

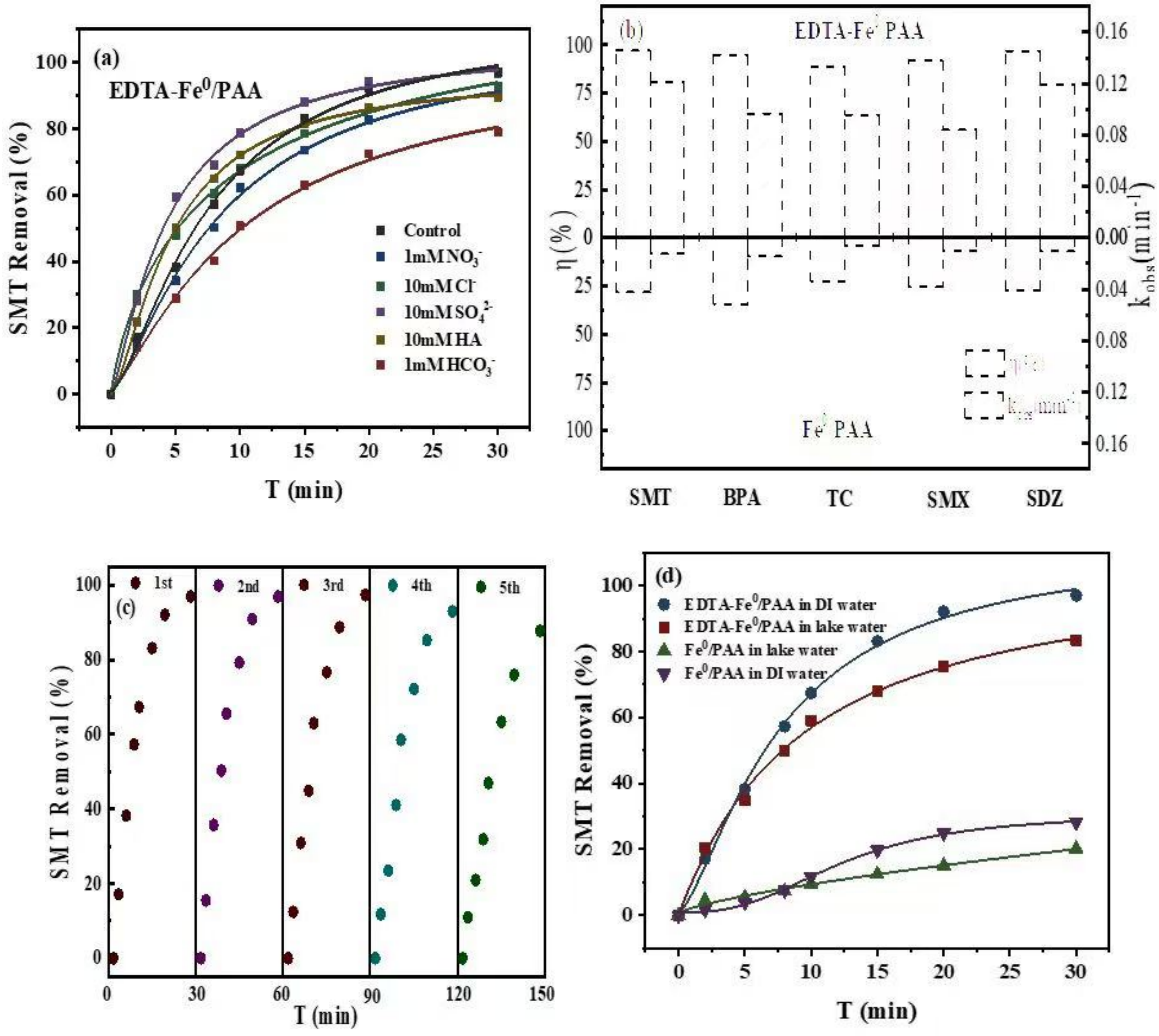

Figure 3 The effect of coexisting inorganic ions and humic acids on the removal of SMT in the EDTA-Fe^0/PAA system (a); The removal efficiency of other antibiotics in the Fe^0/PAA and EDTA-Fe^0/PAA systems (b); The recyclability of surface active agent removal materials in the EDTA-Fe^0/PAA system (c); The removal efficiency of different systems on natural freshwater (d). Reaction condition: antibiotics = 5 mg/L, catalyst = 0.2 g/L, PAA = 0.5 mM, pH = 6.5

4 Conclusion

EDTA-Fe^0 exhibited good catalytic performance, effectively degrading various antibiotic pollutants. The EDTA-Fe^0/PAA composite system demonstrated better performance in removing antibiotics like SDZ, TC, SMX, and BPA compared to the Fe^0/PAA system.

DFT calculations confirmed that EDTA-Fe^0 enhances the activity of PAA, thereby improving antibiotic removal. PAA binds twice as strongly to EDTA-Fe^0 (−0.81 eV) as to bare Fe^0 (−0.41 eV), ensuring faster surface activation.

The degradation of SMT by the EDTA-Fe^0/PAA system produced various intermediate products. The degradation pathway of SMT was inferred based on LC-MS analysis. The toxicity of the intermediates was verified to be relatively low, suggesting that the degradation process is environmentally friendly.

Reference

[1] LIU Yurong, VAN DER HEIJDEN Marcel G A, RIEDO Judith, et al. Soil contamination in nearby natural are as mirrors that in urban greenspaces worldwide[J]. Nature Communications, 2023, 14: 1706.

[2] LI Xi, WANG Shiwen, CHEN Pei, et al. ZIF-derived non-bonding Co/Zn coordinated hollow carbon nitride for enhanced removal of antibiotic contaminants by peroxymonosulfate activation: Performance and mechanism[J]. Applied Catalysis B: Environmental, 2023, 325: 122401.

[3] WU Wentong, ZHANG Lingling, LI Zifu, et al. Research progress of advanced oxidation technology in deg radation of antibiotics and removal of antibiotic resistance[J]. Chemical Industry and Engineering Progre ss, 2021, 40(8): 4551-4561.

[4] XIE Zhihui, HE Chuanshu, PEI Danni, et al. Review of characteristics, generation pathways and detection m ethods of singlet oxygen generated in advanced oxidation processes (AOPs) [J]. Chemical Engineering J ournal, 2023, 468: 143778.

[5] XIE Zhihui, ZHOU Hongyu, HE Chuanshu, et al. Synthesis, application and catalytic performance of l ayered double hydroxide based catalysts in advanced oxidation processes for wastewater decontami nation: A review[J]. Chemical Engineering Journal, 2021, 414: 128713.

[6] DONG Guihua, CHEN Bing, LIU Bo, et al. Advanced oxidation processes in microreactors for water and wastewater treatment: Development, challenges, and opportunities[J]. Water Research, 2022, 211: 118047.

[7] RAYAROTH Manoj P, ARAVINDAKUMAR Charuvila T, SHAH Noor S, et al. Advanced oxidation processes (AOPs) based wastewater treatment-Unexpected nitration side reactions- A serious environmental iss ue: A review[J]. Chemical Engineering Journal, 2022, 430: 133002.

[8] GLAZE William H, KANG Joon-Wun, CHAPIN Douglas H. The chemistry of water treatment processe s involving ozone, hydrogen peroxide and ultraviolet radiation[J]. Ozone: Science & Engineering, 198 7, 9(4): 335-352.

[9] LIU Hongzhi, SHU Xiaoxuan, HUANG Mingjie, et al. Tailoring d-band center of high-valent metal-oxo s pecies for pollutant removal via complete polymerization[J]. Nature Communications, 2024, 15: 2327.

[10] YAN Huijie, PENG Yuan, HUANG Yuyan, et al. Enhancing photosynthesis efficiency of hydrogen pero xide by modulating side chains to facilitate water oxidation at low-energy barrier sites[J]. Advanced Materials, 2024, 36(18): 2311535.

[11] CHEN Yidi, REN Wei, MA Tianyi, et al. Transformative removal of aqueous micropollutants into pol ymeric products by advanced oxidation processes[J]. Environmental Science & Technology, 2024, 58202 5

[12] Zhou Y, Wang T, Zhi D, et al. Applications of nanoscale zero-valent iron and its composites to the removal of antibiotics: a review [J]. Journal of Materials Science, 2019, 54(19): 12171-88.

[13] Lou Y, Cai Y, Tong Y, et al. Interaction between pollutants during the removal of polychlorinated biphenyl-heavy metal combined pollution by modified nanoscale zero-valent iron [J]. Science of The Total Environm ent, 2019, 673: 120-7.

[14] Xu W, Hu X, Lou Y, et al. Effects of environmental factors on the removal of heavy metals by sulfide-modif ied nanoscale zerovalent iron [J]. Environmental Research, 2020, 187: 109662.

[15] Kim J, Zhang T, Liu W, et al. Advanced Oxidation Process with Peracetic Acid and Fe(II) for Contaminant De gradation [J]. Environmental Science & Technology, 2019, 53(22): 13312-22.

[16] Kim J, Du P, Liu W, et al. Cobalt/Peracetic Acid: Advanced Oxidation of Aromatic Organic Compounds by A cetylperoxyl Radicals [J]. Environmental Science & Technology, 2020, 54(8): 5268-78.
[17] Luukkonen T, Heyninck T, Rämö J, et al. Comparison of organic peracids in wastewater treatment: Disinfe ction, oxidation and corrosion [J]. Water Research, 2015, 85: 275-85.
[18] Zhang P, Zhang X, Zhao X, et al. Activation of peracetic acid with zero-valent iron for tetracycline abateme nt: The role of Fe(II) complexation with tetracycline [J]. Journal of Hazardous Materials, 2022, 424: 12765 3.
[19] Shao S, Zhang P, Chen Y, et al. Enhanced tetracycline abatement by peracetic acid activation with sulfidati on of nanoscale zerovalent iron [J]. Environmental Science and Pollution Research, 2023, 30(30): 76157-7 0.
[20] Pan Y, Bu Z, Li J, et al. Sulfamethazine removal by peracetic acid activation with sulfide-modified zero-vale nt iron: Efficiency, the role of sulfur species, and mechanisms [J]. Separation and Purification Technology, 2021, 277: 119402.
[21] He M-F, Li W-Q, Xie Z-H, et al. Peracetic acid activation by mechanochemically sulfidated zero valent iron for micropollutants degradation: Enhancement mechanism and strategy for extending applicability [J]. W ater Research, 2022, 222: 118887.
[22] Wang Z, Wang J, Xiong B, et al. Application of Cobalt/Peracetic Acid to Degrade Sulfamethoxazole at Neut ral Condition: Efficiency and Mechanisms [J]. Environmental Science & Technology, 2020, 54(1): 464-75.
[23] Wang X, Jing J, Zhou M, et al. Recent advances in H2O2-based advanced oxidation processes for removal of antibiotics from wastewater [J]. Chinese Chemical Letters, 2023, 34(3): 107621.
[24] Keen O S, Linden K G. Degradation of Antibiotic Activity during UV/H2O2 Advanced Oxidation and Photoly sis in Wastewater Effluent [J]. Environmental Science & Technology, 2013, 47(22): 13020-30.
[25] Ferro G, Guarino F, Castiglione S, et al. Antibiotic resistance spread potential in urban wastewater effluen ts disinfected by UV/H2O2 process [J]. Science of The Total Environment, 2016, 560-561: 29-35.
[26] Zhao Z, Dong W, Wang H, et al. Advanced oxidation removal of hypophosphite by O3/H2O2 combined wit h sequential Fe(II) catalytic process [J]. Chemosphere, 2017, 180: 48-56.
[27] Matsumoto M, Wada Y, Matsumiya S, et al. Enhanced generation of active oxygen species induced by O3 fine bubble injection under H2O2 addition and UV irradiation [J]. Ozone: Science & Engineering, 2021, 43 (6): 562-70.